Article

Not peer-reviewed version

Driving Naïve State Induction Using Human Wharton Jelly-Mesenchymal Stem Cell-Derived Conditioned Medium in Rhesus Monkey Embryonic Stem Cells

Preeyanan Anwised , Ratree Moorawong , Worawalan Samruan , Jittanun Srisutush , Sirilak Somrednggan , Irene Aksoy , Pierre Savatier * , Rangsun Parnpai *

Posted Date: 26 January 2026

doi: 10.20944/preprints202601.1903.v1

Keywords: conditioned medium; embryonic stem cell; mesenchymal stem cells; primed state; naïve state; rhesus monkey

 doi:10.20944/preprints202601.1903.v1

Article

Driving Naïve State Induction Using Human Wharton Jelly-Mesenchymal Stem Cell-Derived Conditioned Medium in Rhesus Monkey Embryonic Stem Cells

Preeyanan Anwised [1], Ratree Moorawong [1], Worawalan Samruan [1], Jittanun Srisutush [1], Sirilak Somredngan [2], Irene Aksoy [3,4], Pierre Savatier [3,4,*] and Rangsun Parnpai [1,*]

[1] Embryo Technology and Stem Cell Research Center, School of Biotechnology, Institute of Agricultural Technology, Suranaree University of Technology, Nakhon Ratchasima 30000, Thailand

[2] Medeze Group Public Company Limited, Nakhon Pathom 73220, Thailand

[3] Univ Lyon, Université Lyon 1, INSERM, Stem Cell and Brain Research Institute U1208, Lyon, France

[4] PrimaStem Platform, Univ Lyon, Université Lyon 1, INSERM, Stem Cell and Brain Research Institute U1208, Lyon, France

* Correspondence: pierre.savatier@inserm.fr (P.S.); rangsun@g.sut.ac.th (R.P.); Tel.: +33 (0) 472 91 34 42 (P.S.); +66-814706393 (R.P.)

Highlights

- hWJ-MSCs provide a human-compatible, xeno-free alternative to traditional MEFs-based systems.
- hWJ-MSCs promote primed-to-naïve conversion in RhESCs.
- hWJ-MSCs-CM as a novel culture medium for enhancing naïve pluripotency in primate ESCs.
- hWJ-MSCs-CM more robustly induced the expression of key naïve markers, including KLF17, ESRRB, TFAP2C and DPPA2.

Abstract

This study aimed to examine the potential of human Wharton's Jelly-derived mesenchymal stem cells (hWJ-MSCs) in supporting the conversion of the primed state of rhesus monkey embryonic stem cells (rhESCs) to a naïve-like state. The rhESCs were cultured under feeder-free and feeder conditions using hWJ-MSC-conditioned media (hWJ-MSCs-CM) and mouse embryonic fibroblasts CM (MEFs-CM) exhibited distinct morphological changes during conversion. Immunofluorescence analysis demonstrated the expression of pluripotency and naïve markers under both conditions. Gene expression analysis further confirmed the upregulation of naïve-specific genes and downregulation of primed markers, with statistically significant differences between groups. Additionally, epigenetic reprogramming was assessed, revealing differential effects of the CM sources on the reversion to a naïve state. These findings highlight the potential of hWJ-MSCs-CM as a supportive system for naïve-state induction in primate ESCs.

Keywords: conditioned medium; embryonic stem cell; mesenchymal stem cells; primed state; naïve state; rhesus monkey

1. Introduction

In rodents, pluripotent stem cells (PSCs) can transition between two distinct states: the naïve pluripotent state, exemplified by embryonic stem cells (ESCs), and the primed pluripotent state exemplified by epiblast stem cell lines (EpiSCs) [1]. These two states differ markedly in their transcriptional and epigenetic profiles, features that strongly influence their biological characteristics

 doi:10.20944/preprints202601.1903.v1

and functional properties [2]. Historically, human PSCs have existed in a primed-like state, reliant on FGF2 and Activin A to suppress differentiation. Only a few naïve ESC lines have been successfully derived from human blastocysts [3]. Achieving the naïve state typically involves culture in defined cocktails containing growth factors and small-molecule inhibitors (e.g. PKC, MEK, and GSK3β inhibitors). However, the resulting cell lines are often unstable. A more reproducible strategy involves resetting primed ESCs or iPSCs using reprogramming factors that restore naïve-like properties [4–6]. Naïve PSCs also exhibit several functional advantages: they tolerate single cell dissociation and proliferate more rapidly than their primed counterparts. Importantly, they also tend to be more genetically stable, enhancing their utility in genome editing and biomedical applications [2]. However, the efficiency of naïve conversion is highly dependent on culture conditions. Non-human primate (NHPs) ESCs and iPSCs have required more tailored approaches for naïve conversion. Fang et al. (2014) pioneered this in rhesus monkeys using 4i/L/b medium supplemented with LIF, FGF2, and inhibitors targeting MEK, GSK3β, p38MAPK, and JNK, which gradually induced the formation of dome-shaped colonies characteristic of naive PSCs [7]. Other studies reported naïve state reprogramming using increasingly complex cocktails of small molecules: the NHSM/NHSMV cocktail in cynomolgus ESCs [8], and the multi-condition NHSMV/2iLD/K3cLD/K5cLD approach [9]. Bergmann et al. (2022) developed PLAXA medium to reprogram marmoset ESCs (CjESCs) to naïve-like pluripotency using an FGF2/KSR base enriched with MEK and WNT inhibitors, LIF, Activin A, and ascorbic acid [10]. Notably, the 4CL protocol [11], which efficiently converted primed CyESCs to a naïve state with LIF, Activin A, and inhibitors of MEK, tankyrases, S-adenosyl homocysteine hydrolase (SAHH), and histone deacetylases (HDACs), yielding KLF17-enriched, chromosomally stable cells. We recently developed new culture medium, named VALGöX, for converting primed rabbit and NHP iPSCs to the naïve state [12]. This medium consists of fibroblast-conditioned N2B27 supplemented with Vitamin C, LIF, Activin A, the PKC inhibitor Gö6983, and the tankyrase inhibitor XAV939.

Over the past two decades, there has been a growing interest in the development and characterization of conditioned media (CM), particularly in the context of regenerative medicine, where CM is increasingly viewed as a promising cell-free therapeutic product [13]. Most CM used in PSC culture are derived from mouse embryonic fibroblasts (MEFs). On the other hand, mesenchymal stem cells (MSCs), found in various tissues, are multipotent and can differentiate into adipocytes, chondrocytes, and osteocytes [14–16]. Their therapeutic relevance is largely attributed to their immunomodulatory capacity and the secretion of cytokines and growth factors involved in tissue repair and inflammation regulation [15,16]. While CM from MEFs remains widely used, human Wharton's Jelly-derived mesenchymal stem cells-conditioned media (hWJ-MSCs-CM) have emerged as a promising alternative, offering similar support for pluripotent stem cell cultures with lower xenogeneic risks. More recently, hWJ-MSCs-CM has attracted attention as a potential cell-free agent for protective and regenerative therapies [17]. In this study, we evaluated the effectiveness of two different sources of conditioned media—MEFs-CM and hWJ-MSCs-CM—in promoting the conversion of primed rhesus ESCs (rhESCs) to the naïve state. Through morphological assessments, immunofluorescence staining, and gene expression analyses, we compared the capacity of each CM to induce naïve pluripotency features. This work aims to provide new insights for optimizing naïve culture systems in non-human primate ESCs.

2. Materials and Methods

2.1. Chemicals and Reagents

Unless stated otherwise, all chemicals and reagents were purchased from Sigma-Aldrich (St. Louis, Missouri, United States). The cell culture media were purchased from Gibco (Paisley, United Kingdom), and plastic cell culture devices were obtained from SPL Life Sciences (Gyeonggi- do, Republic of Korea).

 doi:10.20944/preprints202601.1903.v1

2.2. Cells and Culture Media

The Rzh11ESC cell line [18] was used in this study. Primed cells were routinely maintained in knockout Dulbecco's modified Eagle's medium (KO-DMEM, Gibco) supplemented with 20% knockout serum replacement (KOSR, Gibco), 1 mM glutamine, 0.1 mM β-mercaptoethanol (Sigma-Aldrich), 1% non-essential amino acids (Gibco), and 4 ng/mL FGF2 (Gibco). Cultures were grown on mitotically inactivated mouse embryonic fibroblasts (MEFs) at a density of 2×10^5 cells per 35-mm dish. Media were changed daily, and cells were passaged every 3–4 days via mechanical dissociation. Mouse embryonic fibroblasts (MEFs) were isolated from 12.5-day-old mouse embryos (Charles River) following the protocol by [19]. Briefly, embryos were dissected, decapitated, and eviscerated. Embryonic tissues were minced and incubated with 5× trypsin for 10 min at 37°C. The digested tissue was centrifuged at 450×g for 10 min, and the cell pellet was resuspended in fibroblast medium (DMEM supplemented with 10% FBS, 1x NEAA, 1% PSG) and plated onto 100-mm dishes. After 2–3 days of culture, MEFs were expanded and cryopreserved at 2×10^6 cells/vial using CryoStor® CS10 medium (Stem Cell Technologies, Vancouver, Canada). Human Wharton's Jelly-derived mesenchymal stem cells (hWJ-MSCs) were obtained via material transfer agreement [20], under ethical approval EC-61-58 (Suranaree University of Technology). Cells were cultured in α-MEM supplemented with 2 mM L-glutamine, 100 U/mL penicillin, 100 µg/mL streptomycin, and 10% fetal bovine serum (FBS).

2.3. hWJ-MSCs Characterization

Colony-Forming Unit (CFU) assay: a total of 200 hWJ-MSCs were seeded per well in 6-well plates and cultured for two weeks with media changes every 2–3 days. Cells were fixed with 4% paraformaldehyde (PFA) for 20 min, stained with 0.5% crystal violet, and examined microscopically (Eclipse Ti-S, Nikon). Colonies (≥50 cells) were manually counted. CFU efficiency was calculated as:

$$\% \text{ CFU} = (\text{Number of colonies} \times 100) / \text{Initial number of seeded cells.}$$

Population Doubling Time (PDT) assay: cells at passages 4–10 was seeded at 4,000 cells/cm² in 35-mm dishes and cultured for 72 h. Viable cells were counted using 0.4% trypan blue.

$$\text{PDT was calculated as: } PDT = (t \times \log 2) / (\log NF - \log NI)$$

where t = time in hours, NI = initial cell number, NF = final cell number.

Flow Cytometry Analysis: hWJ-MSCs (passage 5) were labeled with the following antibodies: CD73-APC, CD90-APC/A750, CD105-PE (Biolegend, 1:100), CD34-PE (Beckman Coulter, 1:10), and CD45-FITC (Biolegend, 1:20). Isotype controls were used. After a 20 min incubation in dark, cells were washed with PBS and analyzed using an Attune™ NxT Flow Cytometer (Thermo Fisher Scientific). Differentiation Assays: cells at passage 5 were cultured on 0.1% gelatin-coated 6-well plates until 80% confluence and induced with lineage-specific media. Osteogenic medium consisted of α-MEM with 100 nM dexamethasone, 0.2 mM ascorbate-2-phosphate, 10 mM β-glycerophosphate; adipogenic medium consisted of α-MEM with 10 µM insulin, 100 µM indomethacin, 1 µM dexamethasone, 0.5 mM IBMX (IBMX removed after 7 days) and chondrogenic medium consisted of α-MEM with 10 µg/mL ITS-X, 50 µg/mL ascorbate-2-phosphate, 40 µg/mL proline, 100 µg/mL sodium pyruvate, 100 nM dexamethasone, 10 ng/mL TGF-β3, and 2% fetal bovine serum (FBS). Media were changed every 3 days over 21 days. Staining included Alizarin Red (osteogenesis), Oil Red O (adipogenesis), and Alcian Blue 8x (chondrogenesis). Cells were visualized by inverted microscopy.

2.4. Conditioned Media Preparation

Cells (MEFs at 4×10^6 and hWJ-MSCs at 3×10^6) at passages 4 and 7, respectively, were treated with 5 µg/mL mitomycin C. Following treatment, the cells were seeded into 10-cm culture dishes and allowed to reach 80–90% confluence in standard culture medium over a period of 24 h. After this incubation, the medium was replaced with 25 mL of N2B27 basal medium supplemented with 20 ng/mL bFGF, and the cells were cultured for an additional 72 h. Conditioned media (CM) were

 doi:10.20944/preprints202601.1903.v1

collected daily, filtered through a 0.2 µm filter, and stored at –20°C until further use. The conditioned media derived from MEFs and hWJ-MSCs are hereafter referred to as MEFs-CM and hWJ-MSCs-CM, respectively.

2.5. Conversion of rhESCs to the Naïve State

Primed colonies were dissociated into single cells using 1×TrypLE™ and subsequently seeded onto two different feeder cell types: MEFs (2.8×10^5 cells per 35 mm dish) and hWJ-MSCs (5.0×10^5 cells per 35 mm dish). The cells were cultured in a mixed medium referred to as VALGöX, which comprised CMs from both OF1-MEFs-CM and hWJ-MSCs-CM, supplemented with 250 µM ascorbic acid, 10 ng/mL Activin A (Peprotech, New Jersey, United States), in-house-produced LIF, 1.25 µM Gö6983 (Bio-Techne, Minnesota, United States), and 2.5 µM XAV939. Cells were maintained at 37°C in a humidified atmosphere containing 5% CO_2 and 5% O_2. The medium was replaced daily, and cells were passaged every three days. On Day 9, the culture medium was switched to ALGöX (identical to VALGöX but without ascorbic acid), and the cells were cultured under this condition until Day 21. For feeder-free culture, cells were seeded onto culture dishes pre-coated with 5 µg/mL laminin-521 (Biolamina, Sundbyberg, Sweden) using the same protocol.

2.6. Immunofluorescence and Imaging

Cells were seeded on 15-mm glass coverslips (Thermo Fisher Scientific, Waltham, United States) before the staining. They were fixed with 4% PFA for 20 min at room temperature (RT), washed three times for 5 min in PBS at RT and permeabilized in 0.5% Triton X-100 for 30 min. After three washes in PBS, cells were kept in blocking solution (2% bovine serum albumin) for 1 h at RT. The cells were then incubated overnight in primary antibodies (1:200 dilution) at 4°C. The following day, cells were washed in PBS and incubated in secondary antibodies (1:200 dilution) for 1 at RT. Cells were then washed three times in PBS prior to mounting in Prolong antifade mounting medium with DAPI (Vector Laboratories, California, United States) and visualized using a fluorescence inverted microscope (Eclipse TE 300, Nikon Imaging Japan Inc.) with NIS-Elements D program (Nikon Imaging Japan Inc., Tokyo, Japan).

2.7. Real-Time Quantitative PCR (qPCR)

Total RNA was extracted using FavorPrep Tissue Total RNA Mini Kit (Favorgen, Ping Tung Biotechnology Park, Taiwan). cDNA synthesis was performed using cDNA Synthesis Kit (Biotechrabbit, Berlin, Germany) and qRT-PCR was performed using KAPA SYBR® FAST qPCR Master Mix on a QuantStudio™ 5 system. Cycling parameters were 95°C for 3 min, followed by 40 cycles of 95°C for 15 sec, 60°C for 30 sec, and 72°C for 30 sec, with a final extension at 72°C for 5 min. Melting curve analysis confirmed primer specificity (Table 1). Gene expression was quantified using the 2^−ΔΔCt method and normalized to GAPDH.

Table 1. Primer sequences and annealing temperatures used for qRT-PCR.

Gene type	Gene	Primer Sequence (5′-3′)	Annealing temperature (°C)
Housekeeping gene	*GADPH*	F: GGAGCGAGATCCCTCCAAAAT R: GGCTGTTGTCATACTTCTCATGG	54
Pluripotency genes	*OCT4*	F: AGTGTGGTTCTGTAACCGGC R: GACCGAGGAGTACAGTGCAG	58
	NANOG	F: AGTCCTGCTTGCAGTTCCAG R: TCAGGTTGCATGTTCGTGGA	55

 doi:10.20944/preprints202601.1903.v1

	SOX2	F: AACCAGCGCATGGACAGTTA R: CGAGCTGGTCATGGAGTTGT	56
Primed specific genes	*TBXT*	F: CTTCAGCAAAGTCAAGCTCACC R: TGAACTGGGTCTCAGGGAAGCA	56
	OTX2	F: AAAGTGAGACCTGCCAAAAAGA R: TGGACAAGGGATCTGACAGTG	56
Naïve specific genes	*KLF4*	F: CCCTACCTCGGAGAGAGACC R: GGATGGGTCAGCGAATTGGA	58
	KLF17	F: CCTTACCGCTGCAACTACGA R: ATAGGGCCTCTCACCTGTGT	57
	TFAP2C	F: GTTCTCAGAAGAGCCAAGTCG R: TCGGCTTCACAGACATAGGC	56
	ESRRB	F: TGCCCTATGACGACAAGCTG R: TGAGCGTCACAAACTCCTCC	58
	DPPA2	F: GTACGCCTGCAGTTTCATGC R: TCTATGCCTGGGGATGGGAA	55
	DPPA5	F: GGTCGTGGTTTACGGTTCCT R: AGTTTGAGCATCCCTCGCTC	56

2.8. Statistical Analysis

All statistical analyses were performed using GraphPad Prism version 5 (GraphPad Software, San Diego, CA, USA). Data are presented as mean ± standard deviation (S.D.). Differences among groups were analyzed using one-way analysis of variance (ANOVA), followed by Tukey–Kramer's Honest Significant Difference (HSD) post hoc test for pairwise comparisons. A p-value of less than 0.05 was considered statistically significant. Graphs were generated using GraphPad Prism version 5.

3. Results

3.1. hWJ-MSC Characterization

The characteristics of hWJ-MSCs were assessed using standard procedures [20]. The colony-forming unit (CFU) assays conducted at passage 4, 5, 6, 7 and 10 yielded values ranging from 16 ± 1.7 to 21.5 ± 3.2 (Figure 1A). The population doubling times (PDts) at passages (P) 4 to 7 and 10 ranged from 38.5 ± 2.2 h to 52.5 ± 5.2 h (Figure 1B), values consistent with those previously reported for hWJ-MSCs derived from human umbilical cord Wharton's jelly [21]. Flow cytometry confirmed that hWJ-MSCs were positive for CD73, CD90, and CD105, and negative for CD34 and CD45 (Figure 1C), with over 95% of cells expressing the positive markers and fewer than 2% expressing the negative markers. Furthermore, hWJ-MSCs demonstrated tri-lineage differentiation potential. Adipogenic differentiation was evidenced by the formation of lipid droplets after 21 days, chondrogenic differentiation by the production of glycosaminoglycan-rich extracellular matrix, and osteogenic differentiation by the appearance of calcium deposits–evidenced using Alizarin Red staining (Figure 1D). All these results are consistent with the criteria set by the International Society for Cell and Gene Therapy [22–24].

 doi:10.20944/preprints202601.1903.v1

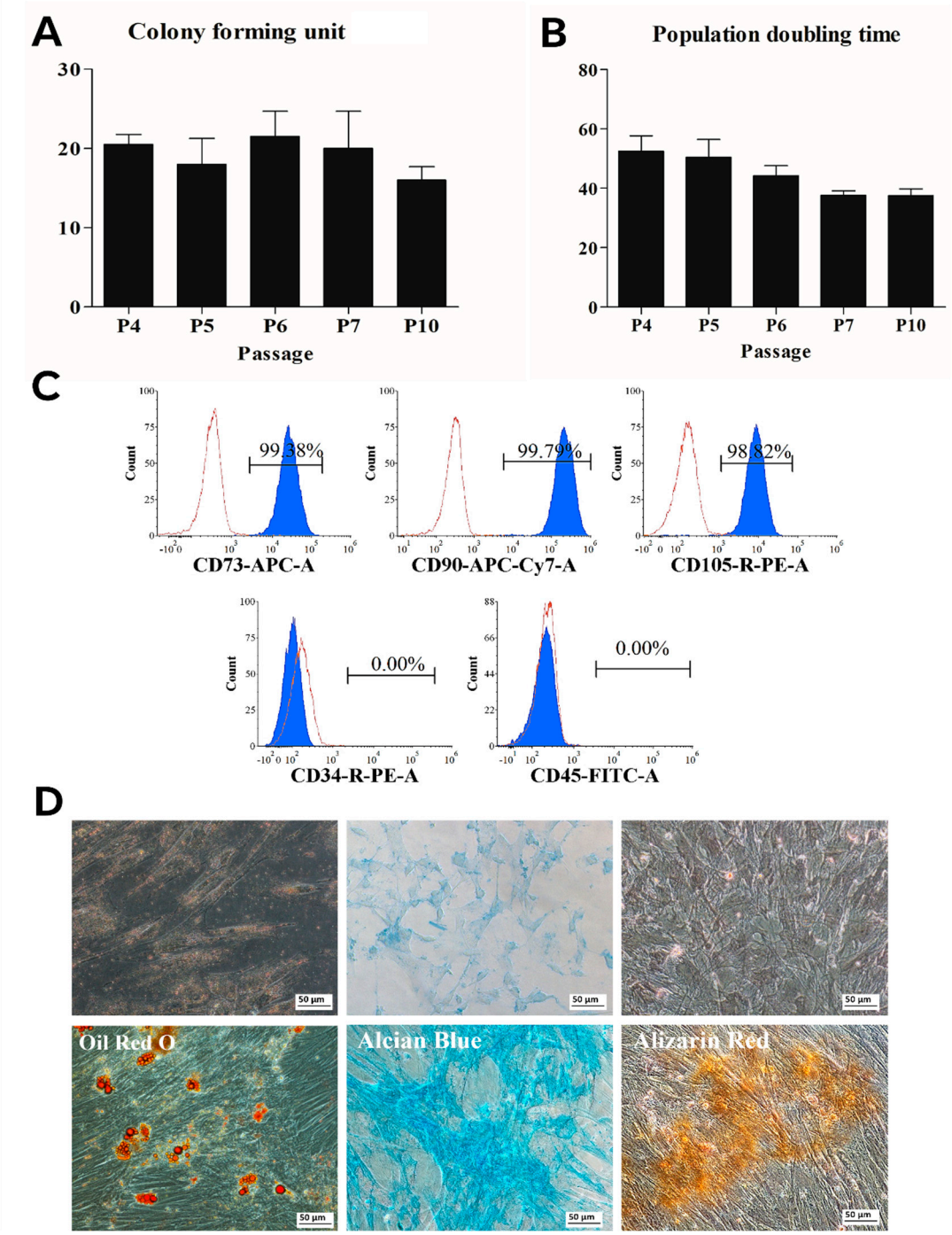

Figure 1. Characterization of hWJ-MSCs. (A) Colony-forming unit assay. (B) Population doubling time. (C) Cell surface expression analyzed by flow cytometry using $CD73^{+}$, $CD90^{+}$, $CD105^{+}$, $CD34^{-}$, and $CD45^{-}$ antibodies. (D) Tri-lineage differentiation potential of hWJ-MSCs after 21 days, assessed by Oil Red O (adipogenesis), Alcian Blue (chrondogenesis), and Alizarin Red (osteogenesis). Scale bar, 50 μm.

3.2. Propagation of Rzh11ESCs Using MEFs and hWJ-MSC-Derived Feeder Cells

The rhesus ESC line Rzh11 (Rzh11ESCs) was originally derived using growth-inactivated MEFs as feeder cells in the presence FGF2 and KOSR, resulting in self-renewal in the primed pluripotent state [18]. In the present study, we found that Rzh11ESCs could also be maintained on feeders derived from hWJ-MSCs. These cells formed flat colonies typical of the primed pluripotency state, demonstrating that hWJ-MSCs-derived feeder cells can support the self-renewal of Rzh11ESCs (Figure 2A). To assess whether hWJ-MSCs-derived feeders could also support self-renewal of

 doi:10.20944/preprints202601.1903.v1

Rzh11ESCs in a naïve-like pluripotent state, we cultured the cells in VALGöX–a medium recently shown to facilitate the conversion of primed rabbit iPSCs to a naïve-like state [12]. Rzh11ESCs were cultured in VALGöX for 9 days on either growth-inactivated MEFs or hWJ-MSCs, followed by 12 days in ALGöX, a modified formulation lacking Vitamin C. Under both feeder conditions, Rzh11ESCs underwent morphological changes indicative of the transition from a flattened, epithelial-like morphology to more compact colonies. Notably, cells cultured on hWJ-MSCs-derived (Day 21) feeders exhibited more pronounced colony condensation and tighter intercellular junctions compared to those on MEFs-derived feeders, suggesting a potentially more rapid induction of naïve characteristics (Figure 2B). By Day 21, Rzh11ESCs on hWJ-MSCs-derived feeders formed well-defined, dome-shaped colonies with smooth borders—morphologies characteristics of the naïve pluripotent state. In contrast, cells cultured on MEFs exhibited partial reprogramming, forming a mixture of flattened and semi-compact colonies, indicative of heterogeneous or incomplete naïve conversion. To further assess the pluripotency status of Rzh11ESCs propagated on MEF- and hWJ-MSCs-derived feeders, we analyzed the expression of key markers by immunofluorescence. Expression of the core pluripotency marker genes OCT4, SOX2, and NANOG remained unchanged between cells maintained in the primed state and those cultured VALGöX/ALGöX on either feeder type (Figure 2C). However, Rzh11ESCs cultured in VALGöX/ALGöX on both feeders showed upregulated expression of naïve pluripotency markers TFAP2C, KDM4A, and KLF17, along with downregulation of the primed marker TBXT (Figure 2D). Additionally, we observed epigenetic changes consistent with the primed-to-naïve transition, including reduced levels of H3K9me3 level and increased levels of H3K14ac at Days 9 and 21 (Figure 2E and 2F). Together, these results demonstrate that hWJ-MSCs-derived feeder cells not only support the self-renewal of Rzh11ESCs in the primed state but also facilitate their conversion to a naïve-like state, as evidenced by morphological and epigenetic changes.

Preprints.org (www.preprints.org) | NOT PEER-REVIEWED | Posted: 26 January 2026 doi:10.20944/preprints202601.1903.v1

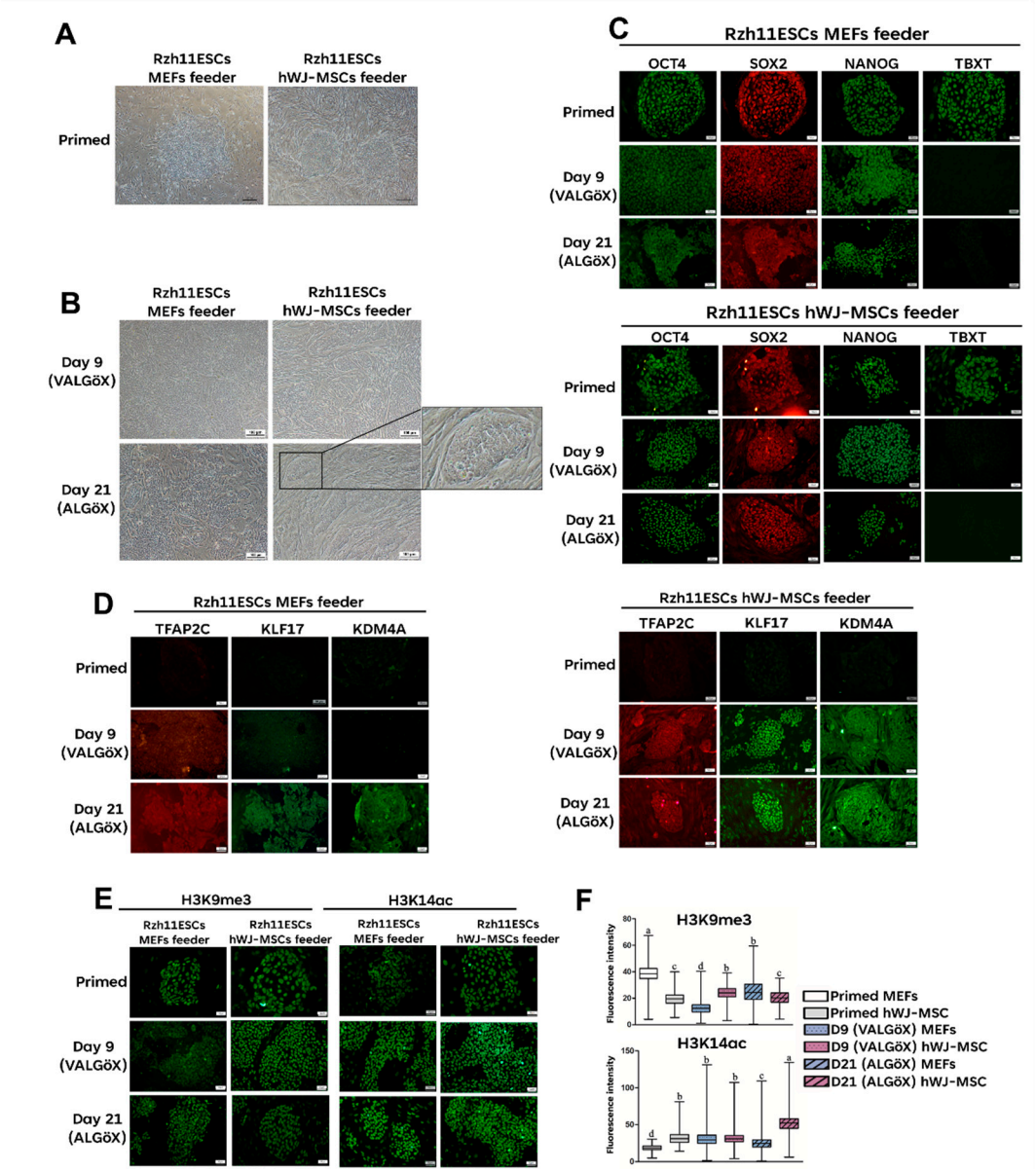

Figure 2. Reversion of Rzh11ESCs from the primed to the naïve-like state using MEFs and hWJ-MSCs feeder cells. (A) Propagation of Rzh11ESCs on MEFs and hWJ-MSCs-derived feeder cells. (B) Morphological changes of Rzh11ESCs in VALGöX/ALGöX medium. (C) Expression of pluripotency markers during the 21-day conversion on feeder cells. (D) Expression of naïve markers during the 21-day conversion on feeder cells. (E) Epigenetic changes during the primed-to-naïve transition. (F) Quantification of epigenetic marker intensities over 21 days. Scale bars: 200 μm (primed Rzh11ESCs), 100 μm (converted Rzh11ESCs), 50 μm (immunofluorescence images).

3.3. Propagation of Rzh11ESCs Using hWJ-MSC-Derived Conditioned Medium

We investigated the capacity of conditioned medium (CM) derived from hWJ-MSCs to support the self-renewal of Rzh11ESCs under feeder-free culture conditions. To this end, Rzh11ESCs initially cultured on MEFs in KOSR/FGF2 were transferred to laminin-521-coated dishes and cultured in VALGöX medium supplemented with either MEFs-CM or hWJ-MSCs-CM for 9 days, followed by 12 days in ALGöX. Under both conditions, Rzh11ESCs maintained an undifferentiated morphology, with no discernable differences in overall appearance. However, significant differences were observed in the pluripotency-associated genes. Immunofluorescence analysis revealed variable expressions of the core pluripotency factors OCT4, NANOG, and SOX2 in Rzh11ESCs transitioned from the primed to the naïve-like state under feeder-free condition (Figure 3A). Notably, cell cultured

 doi:10.20944/preprints202601.1903.v1

in hWJ-MSCs-CM exhibited significantly higher fluorescence intensities. Naïve-specific markers TFAP2C, KDM4A, and KLF17 were upregulated in cells cultured with hWJ-MSCs-CM at both time points, with KDM4A and KLF17 undetectable in the primed state (Figure 3B). Conversely, TBXT expression was markedly downregulated under both CM conditions, further supporting the acquisition of a naïve-like state. Finally, immunofluorescence analysis showed a substantial reduction in H3K9me3 levels in both reversion conditions compared to the primed control, accompanied by a strong increase in H3K14ac expression in converted cells (Figure 3C and D). These findings highlight epigenetic reconfiguration marked by a loss of repressive histone methylation and a gain of permissive histone acetylation. Collectively, these findings underscore the ability of hWJ-MSCs-CM to promote the self-renewal of Rzh11ESCs in a naïve-like state.

 doi:10.20944/preprints202601.1903.v1

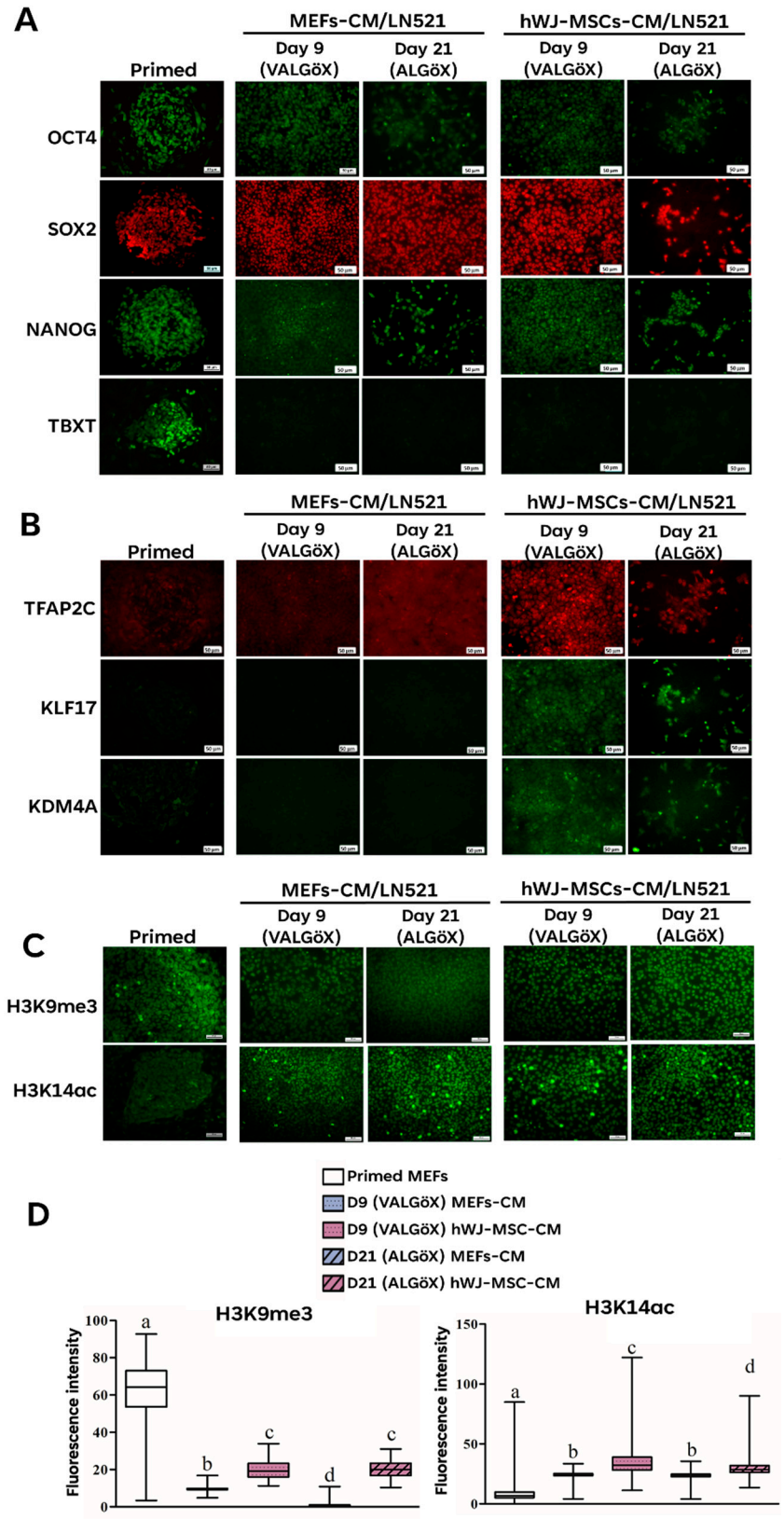

Figure 3. Feeder-free reversion of primed Rzh11ESCs to the naïve state using hWJ-MSCs-condition medium. (A) Expression of pluripotency markers during 21-day conversion on Laminin-521. (B) Expression of naïve markers during 21-day conversion on laminin-521. (C) Epigenetic changes during the primed-to-naïve transition. (D) Quantification of epigenetic marker intensities over 21 days on laminin-521. Scale bars, 50 μm.

3.4. hWJ-MSCs-Derived Conditioned Medium Enhances Primed-to-Naïve State Conversion

 doi:10.20944/preprints202601.1903.v1

We observed that Rzh11ESCs cultured in ALGöX supplemented with hWJ-MSCs-derived CM exhibited higher expression levels of the pluripotency markers TFAP2C, KDM4A, and KLF17 compared to those cultured in MEFs-CM (Figure 3B). This suggests that hWJ-MSCs-CM is more effective in supporting the naïve pluripotent state. To examine this further, we analyzed the expression of naïve pluripotency markers in Rzh11ESCs cultured in ALGöX with either hWJ-MSCs-CM or MEFs-CM using qPCR. The naïve-associated genes KLF4, KLF17, ESRRB, TFAP2C, DPPA2, and DPPA5 were significantly upregulated in both conditions (Figure 4). Notably, cells reprogrammed in hWJ-MSCs-CM exhibited significantly higher expression levels of KLF17, ESRRB, TFAP2C, and DPPA2 compared to those reprogrammed in MEFs-CM, indicating a more robust induction of the naïve transcriptional program.

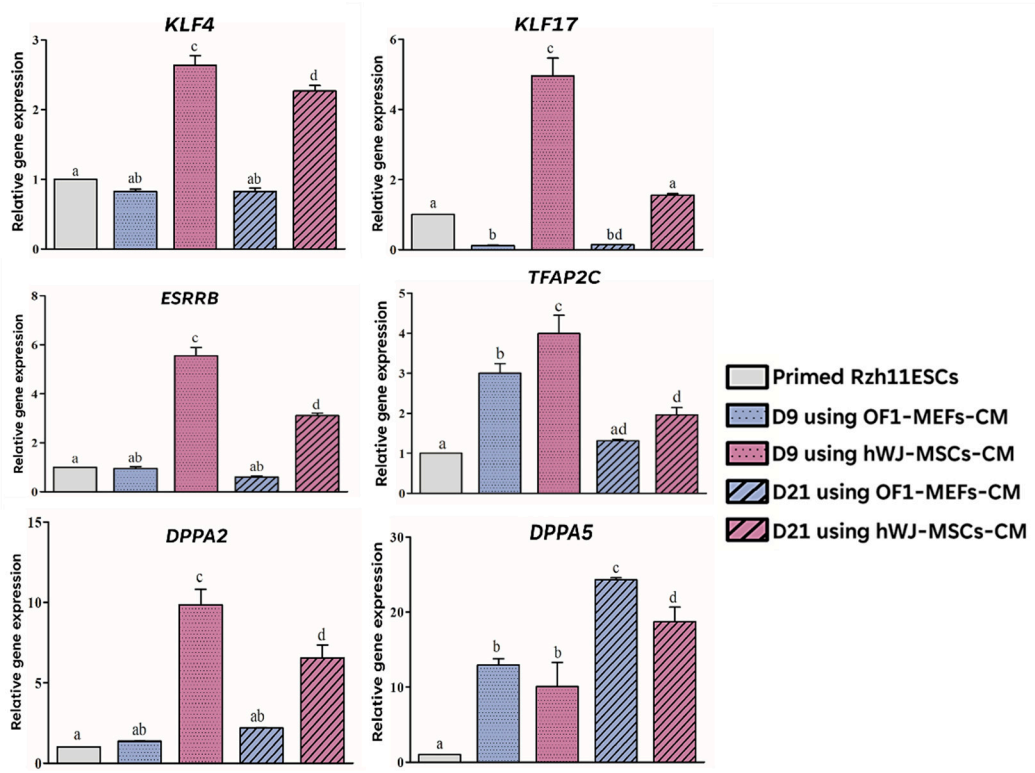

Figure 4. Enhanced primed-to-naïve conversion of Rzh11ESCs by hWJ-MSCs-conditioned medium. Expression levels of naïve markers (KLF4, KLF17, ESRRB, TFAP2C, DPPA2, DPPA5) in Rzh11ESCs cultured with MEFs-CM or hWJ-MSCs-CM. Gene expression was normalized to GAPDH, and relative expression levels were calculated for each group. Data are presented as mean ± S.D. Groups labels with different lowercase letters are significantly different at $p < 0.05$.

4. Discussion

Previous studies have shown that MEF-based feeder systems and their conditioned media can effectively support the reversion of primed human ESCs to a naïve-like state, typically characterized by the upregulation of naïve state-specific transcription factors, including KLF4, KLF17, ESRRB, TFAP2C, DPPA2, and DPPA5, increased acetylation of H3K4 and H3K14, and decreased methylation of K3K9 and H3K27 [25,26]. In our study, we investigated whether feeder cells and conditioned media derived from human Wharton's Jelly mesenchymal stem cells (hWJ-MSCs) could similarly support naïve induction in rhesus ESCs (Rzh11ESCs). Our findings demonstrate that hWJ-MSCs provide a supportive environment for both the maintenance of primed pluripotency and the induction of a naïve-like state, particularly under chemically defined, feeder-free conditions. Interestingly, the expression of naïve markers such as KLF4, KLF17, and DPPA2 was already elevated in Rzh11ESCs cultured on hWJ-MSCs-derived feeders under standard primed conditions. This suggests that hWJ-MSCs may secrete bioactive factors that activate components of the naïve transcriptional network,

 doi:10.20944/preprints202601.1903.v1

even in the absence of naïve-specific culture cues. While hWJ-MSCs are not classically associated with naïve pluripotency induction, their well-characterized secretome—rich in IGF, TGF-β modulators, and other cytokines—may create a paracrine niche conducive to a transitional or "formative-like" pluripotent state [27,28]. This partial activation of naïve-associated pathways was further enhanced under VALGöX/ALGöX culture conditions. Compared to MEFs feeders, hWJ-MSCs-derived feeders support a more rapid and morphologically distinct conversion to the naïve-like state, as evidenced by the formation of dome-shaped colonies and tighter intercellular junctions. These observations suggest that the hWJ-MSCs feeder system not only supports pluripotency but also facilitates epigenetic and morphological transitions characteristic of naïve reprogramming.

The feeder-free experiments using hWJ-MSC-conditioned medium (hWJ-MSC-CM) further highlight the potency of this paracrine environment. Compared to MEFs-CM, hWJ-MSCs-CM more robustly induced the expression of key naïve markers, including KLF17, ESRRB, and DPPA5, alongside significant epigenetic remodeling—namely, reduced H3K9me3 and increased H3K14ac levels. These changes are consistent with chromatin states permissive to naïve gene activation and suggest that hWJ-MSCs-CM not only initiates transcriptional reprogramming but also promotes chromatin accessibility in line with naïve identity. A notable morphological difference is also observed between the two conditioned media: Rzh11ESCs cultured in hWJ-MSCs-CM exhibited larger cell size relative to those in MEFs-CM. Naïve pluripotent cells are known to display a unique metabolic and cytoskeletal profile, including increased mitochondrial activity and cytoplasmic spreading [29,30]. The increased size of hWJ-MSCs-CM-cultured cells may thus reflect a shift in metabolic state or cytoskeletal organization associated with naïve conversion.

Taken together, these results support the conclusion that hWJ-MSCs, through both direct contact and secreted factors, contribute to a permissive microenvironment for the induction and maintenance of a naïve-like pluripotent state. While the transition may not be fully complete in all cells, the consistent upregulation of naïve-associated transcription factors and accompanying epigenetic modifications point to the activation of a functional naïve gene network. Moreover, hWJ-MSCs provide a human-compatible, xeno-free alternative to traditional MEFs-based systems, with important implications for regenerative medicine and interspecies chimerism studies.

Author Contributions: Conceptualization, P.A., and R.P.; methodology, P.A., R.M., W.S., and S.S.; software, P.A., R.M., W.S.; validation, P.A., and R.P.; formal analysis, P.A., W.S., S.S.; investigation, W.S., S.S., J.S., and R.P.; resources, R.P. and P.S.; data curation, P.A., R.M. and W.S.; writing—original draft preparation, P.A., W.S.; writing—review and editing, P.A., W.S., I.A., P.S., and R.P.; visualization, P.A., W.S., S.S.; supervision, I.A., P.S., and R.P.; project administration, P.A., and R.P.; funding acquisition, R.P., and P.S. All authors have read and agreed to the published version of the manuscript.

Funding: This research was supported by funding from the National Science, Research and Innovation Fund (NSRF) through the Program Management Unit for Human Resources & Institutional Development, Research and Innovation (PMU-B), Government of Thailand (Grant Number: B16F640104); Suranaree University of Technology (SUT); Franco-Thai Mobility Programme/PHC SIAM, Year 2023-2024 to Rangsun Parnpai and Irene Aksoy. Preeyanan Anwised was supported by SUT full-time postdoctoral researchers. Worawalan Samruan was supported by SUT full-time postdoctoral researchers.:

Institutional Review Board Statement: The animal study protocol was approved by Ethics Committee of Institutional Animal Care and Use Committee, Suranaree University of Technology (protocol code EC-61-58).

Informed Consent Statement: Not applicable.

Data Availability Statement: The data presented in this study is available on request from the corresponding author.

Acknowledgments: We thank the Yerkes National Primate Research Center (Atlanta, GA, USA) for granting consent to use the Rzh11 embryonic stem cell line in our experiments. We are also grateful to the Embryo Technology and Stem Cell Research Center (ESRC), School of Biotechnology, Institute of Agricultural

 doi:10.20944/preprints202601.1903.v1

Technology, Suranaree University of Technology, for their generous support in providing essential laboratory equipment.

Conflicts of Interest: The authors declare that they have no conflicts of interest in this work.

Abbreviations

The following abbreviations are used in this manuscript:

bFGF	Basic fibroblast growth factor
CjESCs	Marmoset ESCs
CyESCs	Cynomolgus monkey
CFU	Colony-Forming Unit
ESCs	Embryonic stem cells
EpiSCs	Epiblast stem cells
FBS	Fetal bovine serum
NHPs	Non-human primates
HDACs	Histone deacetylases
hWJ-MSCs	Human Wharton's Jelly-derived mesenchymal stem cells
hWJ-MSCs-CM	hWJ-MSC-conditioned media
KO-DMEM	Knockout Dulbecco's modified Eagle's medium
KOSR	Knockout serum replacement
MEFs	Mouse embryonic fibroblasts
MEFs-CM	MEFs-conditioned media
PSCs	Pluripotent stem cells
rhESCs	Rhesus monkey embryonic stem cells
RT	Room temperature
PFA	Paraformaldehyde
SAHH	S-adenosyl homocysteine hydrolase

References

1. Nichols, J.; Smith, A. Naïve and primed pluripotent states. *Cell Stem Cell.* **2009**, *4*, 487–492. https://doi.org/10.1016/j.stem.2009.05.015.
2. Weinberger, L.; Ayyash, M.; Novershtern, N.; Hanna, J.H. Dynamic stem cell states: Naïve to primed pluripotency in rodents and humans. *Nat. Rev. Mol. Cell Biol.* **2016**, *17*, 155–169. https://doi.org/10.1038/nrm.2015.28.
3. Guo, G.; von Meyenn, F.; Santos, F.; Chen, Y.; Reik, W.; Bertone, P.; Smith, A.; Nichols, J. Naive pluripotent stem cells derived directly from isolated cells of the human inner cell mass. *Stem Cell Reports*. **2016**, *6*, 437–446. https://doi.org/10.1016/j.stemcr.2016.02.005.
4. Wang, Y.; Zhao, C.; Hou, Z.; Yang, Y.; Bim, Y.; Wang, H.; Zhang, Y.; Gao, S. Unique molecular events during reprogramming of human somatic cells to induced pluripotent stem cells (iPSCs) at naïve state. *Elife*. **2018**, *30*, 7:e29518. https://doi.org/10.7554/eLife.29518.
5. Giulitti, S.; Pellegrini, M.; Zorzan, I.; Martini, P.; Gagliano, O.; Mutarelli, M.; Ziller, M.J.; Cacchiarelli, D.; Romualdi, C.; Elvassore, N. et al. Direct generation of human naive induced pluripotent stem cells from somatic cells in microfluidics. *Nat. Cell Biol*. **2019**, *21*, 275–286. https://doi.org/10.1038/s41556-018-0254-5.
6. Buckberry, S.; Liu, X.; Poppe, D.; Tan, P.J.; Sun, G.; Chen, J.; Nguyen, T.V.; de Mendoza, A.; Pflueger, J.; Frazer, T.; et al. Transient naive reprogramming corrects hiPS cells functionally and epigenetically. *Nature*. **2023**, *620*, 863–872. https://doi.org/10.1038/s41586-023-06424-7.
7. Fang, R.; Liu, K.; Zhao, Y.; Li, H.; Zhu, D.; Du, Y.; Xiang, C.; Li, X.; Liu, H.; Miao, Z.; et al. Generation of naive induced pluripotent stem cells from rhesus monkey fibroblasts. *Cell Stem Cell*. **2014**, *15*, 488–497. https://doi.org/10.1016/j.stem.2014.09.004.
8. Chen, Y.; Niu, Y.; Li, Y.; Ai, Z.; Kang, Y.; Shi, H.; Xiang, Z.; Yang, Z.; Tan, T.; Si, W.; et al. Generation of Cynomolgus Monkey Chimeric Fetuses using Embryonic Stem Cells. *Cell Stem Cell*. **2015**, *17*, 116–124. https://doi.org/10.1016/j.stem.2015.06.004.

9. Honda, H.; Kawano, Y.; Izu, H.; Choijookhuu, N.; Honsho, K.; Nakamura, T.; Yabuta, Y.; Yamamoto, T.; Takashima, Y.; Hirose, M., et al. Discrimination of Stem Cell Status after Subjecting Cynomolgus Monkey Pluripotent Stem Cells to Naïve Conversion. *Sci Rep.* **2017**, *7*, 45285. https://doi.org/10.1038/srep45285.
10. Bergmann, S.; Penfold, C.A.; Slatery, E.; Siriwardena, D.; Drummer, C.; Clark, S.; Strawbridge, S.E.; Kishimoto, K.; Vickers, A.; Tewary, M.; et al. Spatial profiling of early primate gastrulation in utero. *Nature*. **2022**, *609*, 136–143. https://doi.org/10.1038/s41586-022-04953-1.
11. Li, J.; Zhu, Q.; Cao, J.; Liu, Y.; Lu, Y.; Sun, Y.; Li, Q.; Huang, Y.; Shang, S.; Bian, X.; et al. Cynomolgus monkey embryo model captures gastrulation and early pregnancy. *Cell Stem Cell* **2023**, *30*, 362–377. https://doi.org/10.1016/j.stem.2023.03.009.
12. Pham, H.T.; Perold, F.; Pijoff, Y.; Doerflinger, N.; Rival-Gervier, S.; Givelet, M.; Moulin, A.; Ressaire, M.; Da Silva Fernandes, E.; Bidault, V.; et al. Efficient generation of germline chimeras in a non-rodent species using rabbit induced pluripotent stem cells. *Nat. Commun.* **2025**, *16*, 5165. https://doi.org/10.1038/s41467-025-60314-2.
13. Kuo, S.C.; Chio, C.C.; Yeh, C.H.; Ma, J.T.; Liu, W.P.; Lin, M.T.; Lin, K.C.; Chang, C.P. Mesenchymal stem cell-conditioned medium attenuates the retinal pathology in amyloid-β-induced rat model of Alzheimer's disease: Underlying mechanisms. *Aging Cell*. **2021**, *20*, e13340. https://doi.org/10.1111/acel.13340.
14. da Silva Meirelles, L.; Chagastelles, P.C.; Nardi, N.B. Mesenchymal stem cells reside in virtually all post-natal organs and tissues. *J. Cell Sci*. **2006**, *119* ,2204-2213. https://doi.org/10.1242/jcs.02932.
15. Chamberlain, G.; Fox, J.; Ashton, B.; Middleton, J. Concise review: mesenchymal stem cells: their phenotype, differentiation capacity, immunological features, and potential for homing. *Stem Cells*. **2007**, *25*, 2739-2749. https://doi.org/10.1634/stemcells.2007-0197.
16. Abbasi-Malati, Z.; Roushandeh, A.M.; Kuwahara, Y.; Roudkenar, M.H. Mesenchymal Stem Cells on Horizon: A New Arsenal of Therapeutic Agents. *Stem Cell Rev Rep*. **2018**, *14*, 484-499. https://doi.org/10.1007/s12015-018-9817-x.
17. Acuto, S.; Lo Iacono, M.; Baiamonte, E.; Lo Re, R.; Maggio, A.; Cavalieri, V. An optimized procedure for preparation of conditioned medium from Wharton's jelly mesenchymal stromal cells isolated from umbilical cord. *Front Mol Biosci*. **2023**, *2*, 10:1273814. https://doi.org/10.3389/fmolb.2023.1273814.
18. Putkhao, K.; Kocerha, J.; Cho, I.K.; Yang, J.; Parnpai, R.; Chan, A.W. Pathogenic cellular phenotypes are germline transmissible in a transgenic primate model of Huntington's disease. *Stem Cells Dev*. **2013,** *22*, 1198-1205. https://doi.org/10.1089/scd.2012.0469.
19. Afanassieff, M.; Tapponnier, Y.; Savatier, P. Generation of Induced Pluripotent Stem Cells in Rabbits. *Induced Pluripotent Stem (iPS) Cells. Methods and Protocols*, 2nd ed.; Turksen, K., Nagy, A., Eds.; Humana Press: New York, NY, USA, 2014; Volume 1357, pp. 149–172. https://doi.org/10.1007/7651_2014_140.
20. Somredngan, S.; Theerakittayakorn, K.; Nguyen, H.T.; Ngernsoungnern, A.; Ngernsoungnern, P.; Sritangos, P.; Ketudat-Cairns, M.; Imsoonthornruksa, S.; Keeratibharat, N.; Wongsan, R.; Rungsiwiwut, R.; Parnpai, R. The Efficiency of Neurospheres Derived from Human Wharton's Jelly Mesenchymal Stem Cells for Spinal Cord Injury Regeneration in Rats. *Int J Mol Sci*. **2023**, *24*, 3846. https://doi.org/10.3390/ijms24043846.
21. Bharti, D.; Shivakumar, S.B.; Park, J.K.; Ullah, I.; Subbarao, R.B.; Park, J.S.; Lee, S.L.; Park, B.W.; Rho, G.J. Comparative analysis of human Wharton's jelly mesenchymal stem cells derived from different parts of the same umbilical cord. *Cell Tissue Res*. **2018**, *372*, 51-65. https://doi.org/10.1007/s00441-017-2699-4.
22. Wang, H.S.; Hung, S.C.; Peng, S.T.; Huang, C.C.; Wei, H.M.; Guo, Y.J.; Fu, Y.S.; Lai, M.C.; Chen, C.C. Mesenchymal stem cells in the Wharton's jelly of the human umbilical cord. *Stem Cells*. **2004**, *22*, 1330-1337. https://doi.org/10.1634/stemcells.2004-0013.
23. Dominici, M.; Le Blanc, K.; Mueller, I.; Slaper-Cortenbach, I.; Marini, F.; Krause, D.; Deans, R.; Keating, A.; Prockop, Dj.; Horwitz, E. Minimal criteria for defining multipotent mesenchymal stromal cells. The International Society for Cellular Therapy position statement. *Cytotherapy*. **2006**, *8*, 315-7. https://doi.org/10.1080/14653240600855905.
24. Fong, C.Y.; Subramanian, A.; Gauthaman, K.; Venugopal, J.; Biswas, A.; Ramakrishna, S.; Bongso, A. Human umbilical cord Wharton's jelly stem cells undergo enhanced chondrogenic differentiation when grown on nanofibrous scaffolds and in a sequential two-stage culture medium environment. *Stem Cell Rev Rep*. **2012**, *8*, 195-209. https://doi.org/10.1007/s12015-011-9289-8.

 doi:10.20944/preprints202601.1903.v1

25. Bates, L.E.; Silva, J.C. Reprogramming human cells to naïve pluripotency: how close are we? *Curr Opin Genet Dev*. **2017**, *46*, 58-65. https://doi.org/10.1016/j.gde.2017.06.009.
26. Zhou, J.; Hu, J.; Wang, Y.; Gao, S. Induction and application of human naive pluripotency. *Cell Rep*. **2023**, *42*, 112379. https://doi.org/10.1016/j.celrep.2023.112379.
27. Hanna, J.; Cheng, A.W.; Saha, K.; Kim, J.; Lengner, C.J.; Soldner, F.; Cassady, J.P.; Muffat, J.; Carey, B.W.; Jaenisch, R. Human embryonic stem cells with biological and epigenetic characteristics similar to those of mouse ESCs. *Proc Natl Acad Sci U S A*. **2010**, 107, 9222-9227. https://doi.org/10.1073/pnas.1004584107.
28. Batsivari, A., Haltalli, M.L.R., Passaro, D.; Pospori, C.; Celso, C.L.; Bonnet, D. Dynamic responses of the haematopoietic stem cell niche to diverse stresses. *Nat Cell Biol.* **2020**, *22*, 7–17. https://doi.org/10.1038/s41556-019-0444-9.
29. Theunissen, T.W.; Powell, B.E.; Wang, H.; Mitalipova, M.; Faddah, D.A.; Reddy, J.; Fan, Z.P.; Maetzel, D.; Ganz, K.; Shi, L.; et al. Systematic identification of culture conditions for induction and maintenance of naive human pluripotency. *Cell Stem Cell*. **2014**, *15*, 471-487. https://doi.org/10.1016/j.stem.2014.07.002.
30. Buecker, C.; Srinivasan, R.; Wu, Z.; Calo, E.; Acampora, D.; Faial, T.; Simeone, A.; Tan, M.; Swigut, T.; Wysocka, J. Reorganization of enhancer patterns in transition from naive to primed pluripotency. *Cell Stem Cell*. **2014**, *14*, 838-853. https://doi.org/10.1016/j.stem.2014.04.003.